

Concentration effects on the IR-luminescent channels for Er- and Ho-doped LiYF₄ crystals

Mary B. Camargo^a, Laercio Gomes, Izilda M. Ranieri

^a Instituto de Física de Universidade Federal do Rio de Janeiro, Caixa Postal 11098, Maracanã, 05421-970 São Paulo, Brazil

Received 12 February 1996; accepted 17 July 1996

Abstract

In this paper we report the ideal concentrations for the main infrared laser channels of the Er³⁺ and Ho³⁺-doped LiYF₄ (YLF) crystals, under Xe lamp pumping. The number of photons per luminescent element are also obtained for each laser. It was determined that 10–30% of Er ions at wt is the ideal concentration for laser action at 2.74 μm , as well as the 1.2% Er-doped YLF crystal is the best one for lasing at 0.88, 1.23, and 1.72 μm under flashlamp pumping. The proposed method is a good approach in order to indicate the ideal concentration for an optimized four-level laser system. For the transitions at 1.63 μm (Er:YLF) and at 2.07 μm (Ho:YLF) it was observed that the luminescence intensities are maximized in the concentration range (25–35)% for Er ions and in the range (10–15)% for Ho ions in the YLF crystals. However, these concentration values are much higher than the ones used in a practical three-level laser system.

1. Introduction

The lasers based on the rare-earth (RE³⁺) ion transition in crystals are very useful for a large number of applications in industry, [1–4] science, [5,6] medicine, [7–10] communications, fibre and air defence [11,12]. Among these lasers, the ones based on Er³⁺ and Ho³⁺ are important because of their laser transitions, which run from 0.80 to 3.00 μm . The overlapping of the water absorption spectrum with these laser emission at 2.74 μm (Er:YLF) and 2.07 μm (Ho:YLF), makes these very convenient as medical tools for cutting, ablation, and other medical procedures where the laser interacts directly with the

biological tissues, whose composition is mostly water.

In a previous work, we studied the temperature dependence of the Er- and Ho-ion luminescence in LiYF₄ crystals [13,14] for low and high doping concentration. Pumping the ⁴G_{11/2} manifold of low Er-concentration crystals at 77 K, the most intense luminescences are: ⁴S_{3/2} → ⁴I_{13/2} at 546 nm and ⁴S_{3/2} → ⁴I_{15/2} at 647 nm. On the other hand, at a higher concentration (38.5%), those transitions are quenched by both temperature (room temperature) and concentration and therefore, the other mid-infrared luminescent channels, beyond 850 nm, are the main contributors to the total luminescence of that laser material. For the Ho:YLF crystals, the high concentration affects intensities the quenching of the visible transitions favouring the transitions at 1.3 μm (²I₈ → ²I₅) and at 2.1 μm (²I₇ → ²I₅).

^a Corresponding author.

Although that previous work demonstrated how temperature and a drastic change in the dopant concentration affects the luminescence of these laser materials, the effect of the activator concentration variation on the luminescence of the main laser transitions of Er^{3+} and Ho^{3+} ions in LiYF_4 crystals were not investigated.

Pumping the Er and the Ho:LiYF_4 crystals with the white light from a Xe flashlamp, one determines the crystal behavior under a flashlamp pumped laser resonator, where almost all the transitions of the activator are excited (see Fig. 1 for the Er:LiYF_4). In the present work, the active ion (Er , Ho) concentration in the YLF crystals was varied, keeping the same pumping conditions in order to verify the laser concentrations for each laser transition.

In order to make it clear that the absorption does in this work is valid an isolated another figure (Fig. 2), showing the spectrum of our Xe cw lamp (Cermet Xe, model LX300UV, 950 W) with an IR filter

(Solex glass KG-3) and also that one referring to a common ILC Xe flashlamp [15] with a current density of 3100 A/cm^2 and gas pressure of 450 Torr [16], used to pump erbium lasers. The KG-3 filter cuts all wavelengths below 300 nm and above 1000 nm. This filter was used together with the Xe lamp, to simulate a flashlamp pumped water cooled laser resonator because the thin film of water which works as a filter for the UV and IR ($> 1000 \text{ nm}$) wavelengths. It is important to notice that the flashlamp with the thin film of water presents almost the same spectrum than the one realized by the pumping system used in the present work.

2. Experiment

A conventional hydrofluorination procedure utilizing ultra pure rare earth oxides was used to synthesize the coating materials for the crystal probes. The

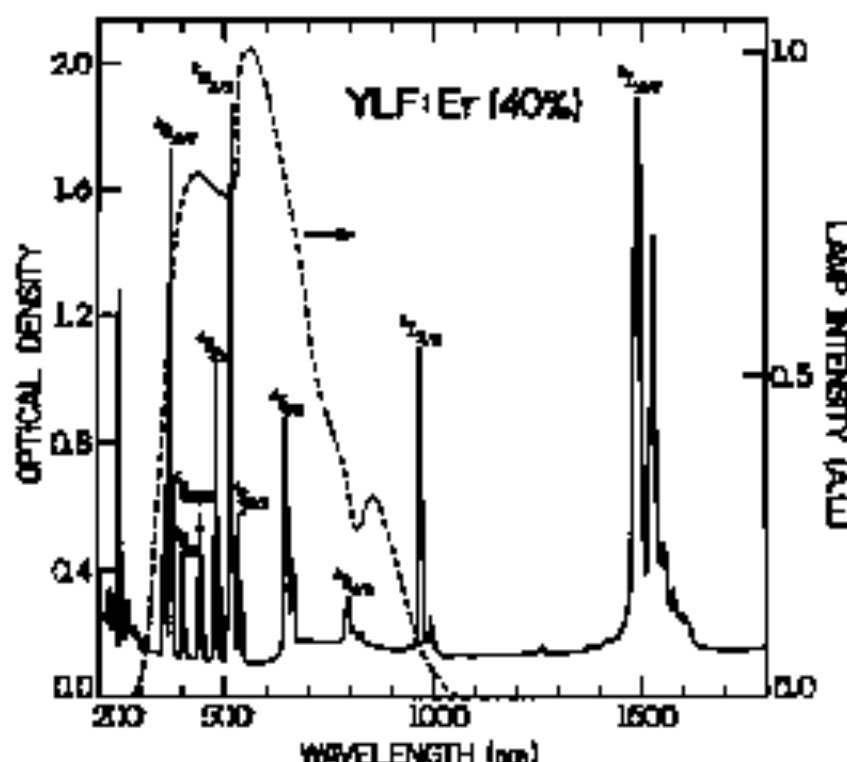


Fig. 1. $\text{OH:LiYF}_4/\text{YLF}$ absorption spectrum at 300 K, referring to the left axis and the Xe lamp plus an IR filter (cut-off at 1000 nm) spectrum which was used to pump the YLF crystals, referring to the right axis. 30.3% was the measured value for the Er-concentration in the crystal.

Er or Ho:YLF synthesized material was grown by conventional Czochralski's method under argon atmosphere. Both Ho and Er:YLF basals underwent a thermal treatment prior to sample preparation, in eliminate the stress originated during the growth process. Er doped YLF could be grown in special concentrations from 1 to 100%. On the other hand, during the Ho:YLF crystal growth, the bismuth fluoride (BiF_3) could be added to the YLF melt forming a solid solution up to 10% at wt. For higher Ho concentrations, however, there is a solubility precipitation due to the YF_3 - HoF_3 phase-diagram incongruence; in spite of that the Ho:YLF could be obtained.

After the crystal growth, we selected the regions of the boules free of scattering to collect the samples. The samples used in this study were single crystals of Ho:YLF and Er:YLF with variable RE^{3+} ion concentration (1.00, 1.42, 2.77, 4.55, 38.5, and 100% for Er crystals and 1.71, 3.00, 7.00 and 100% for Ho crystals). 2.7 mm thick Er:YLF and 2.0 mm thick Ho:YLF crystals were cut and polished with parallel surfaces for that purpose.

The experimental setup is the same as described

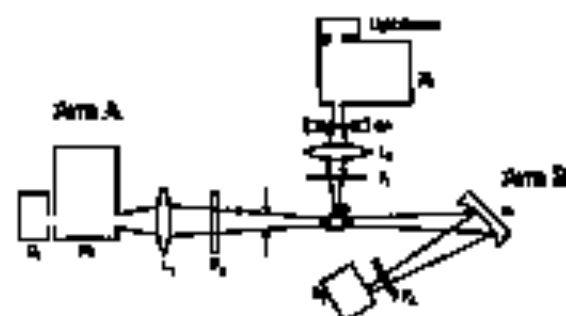


Fig. 3. Experimental setup. D₁ and D₂ are detectors (PMT and/or SiPM), M₁ and M₂ are monochromators, R is a rotator, S is the sample, L₁ and L₂ are lenses, F₁ is a EG-5 glass filter with a cut-off at 300 nm and F₂ is a 200 nm or a 20 nm wide filter, F₃ is a 2 mm thick CaF₂ window filter, and W is a vacuum window (W-10 and lens curve radius = 15 cm).

in section [13] (see Fig. 3). The excitation was provided by the stabilized constant current Xe commercial LX500UV plus the EG-5 glass filter, described earlier in the text. In order to minimize the stray-light contribution to the measured signal, the measurements were taken at 90° from the excitation light-beam. To perform quantitative luminescence

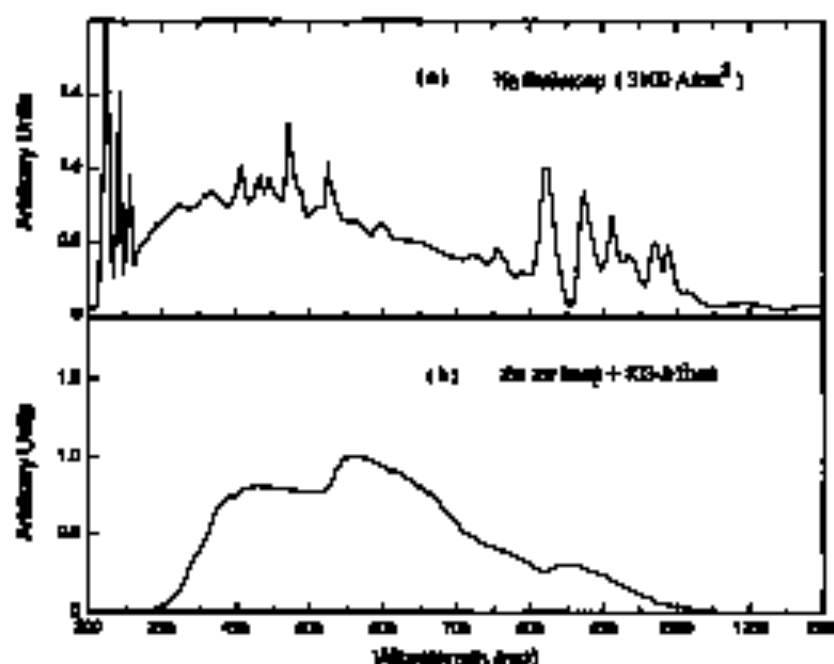


Fig. 2. Comparison between the spectra of: (a) a detection E.C. Ho:Ho:YLF (300 μm^2 that had 3100 A/cm^2) used to pump 100% Ho:YLF and (b) a Chinese experiment Ho:YLF (300 μm^2) used to pump Ho:YLF crystals in this work.

transmission, the excitation and collecting optics in the sample under investigation were kept the same. All the fluorescence, for $\lambda \leq 2.6 \mu\text{m}$, were measured in arm A by using a system composed by a filter F_1 (RG780 or Si filter), a Koflex analyser monochromator (0.25 m) with slit of 1 mm and a detector D_1 (S-20 extended, S-1 FMT's from EMI or InGa from Jasco). These slit were chosen so match the integration interval to the multiple width under investigation. The only luminescent channel observed in arm B was 2.74 μm because this luminescence was too weak to be observed in arm A. In this case, a collecting mirror was used to focus the light into a detector and a Ge filter was used in front of the detector D_2 (InGa, Jasco's J10 series), which was cooled at 77 K. The responsivity of all the detectors (in V/W) was obtained using an electrically calibrated pyroelectric radiometer model RS-5900 from Labs Precision, as a reference.

The transmission band-pass of the analyser monochromator was taken for each luminescent channel in

TABLE I

Filters used in the experimental setup and the slit where the measurement was taken.

Fluorescence group (μm)	Where slit	Slit transmission T (%)	Arm
880–930	RG 780	85	A
1050–2000	Si	50	A
Flu On Er acac/acac at 2746 nm	Ge	45	B

order to correct the values of the luminescence signals. It was a Gaussian shape with a half-width of 12 nm.

The luminescence power, corrected and normalized for each luminescent channel, in W/cm², was obtained using the expression:

$$\beta = \frac{S_1 \beta T}{S T} \quad (1)$$

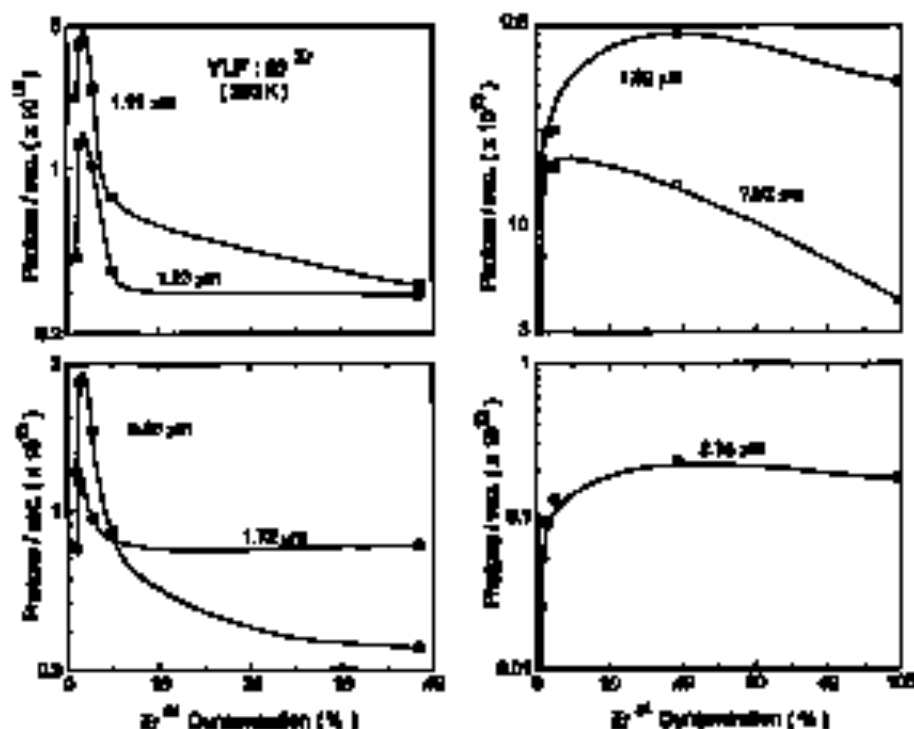


Fig. 4. Decay of photorefractive index by the Er^{3+} in concentrations, as a function of Er-concentration, the On Er:LYE crystals for a 20 mW excitation at 880 nm. The curves correspond to the following Er^{3+} transitions: 1.83 μm (${}^4\text{F}_{3/2} \rightarrow {}^4\text{I}_{13/2}$), 1.85 μm (${}^4\text{F}_{3/2} \rightarrow {}^4\text{I}_{15/2}$), 1.88 μm (${}^4\text{F}_{3/2} \rightarrow {}^4\text{I}_{13/2}$), 1.91 μm (${}^4\text{F}_{3/2} \rightarrow {}^4\text{I}_{15/2}$), 1.93 μm (${}^4\text{F}_{3/2} \rightarrow {}^4\text{I}_{13/2}$), 1.95 μm (${}^4\text{F}_{3/2} \rightarrow {}^4\text{I}_{15/2}$), 1.98 μm (${}^4\text{F}_{3/2} \rightarrow {}^4\text{I}_{13/2}$), 2.00 μm (${}^4\text{F}_{3/2} \rightarrow {}^4\text{I}_{15/2}$) and 2.74 μm (${}^4\text{I}_{13/2} \rightarrow {}^4\text{I}_{15/2}$).

where S_i is the measured integrated luminescence signal (in V), p is a correcting factor (defined in Eq. (2)) which takes into account the transmission band-pass of the analyzer monochromator T_i , and g is the ratio between the area under the 4π and the one used in eqn A (in B). R is the detector sensitivity (in V/W) and T is the optical transmission of the optical filter used in the experiment. In this context for the integrated luminescence signal measurement correction (β), the main source of errors are the factors p and g . As a consequence, a typical error of 0% must be considered.

The filter used in the experimental setup as well as the collecting arm, whose data were taken, are indicated in Table 1. The KG-3 glass filter, with a cut-off at 1.0 μm , was placed in the excitation light beam path in order to simulate the excitation spectrum of a Xe flashlamp typically used to pump a laser rod inside a laser resonator. The Xe lamp spectrum with the KG-3 glass filter can be seen in Figs. 1 and 2.

The factor g is defined as the ratio between the corrected luminescence signal and the measured one:

$$p = \frac{\sum_i S_i \Delta(\lambda_i)}{\sum_i S_i T_i \Delta(\lambda_i)}, \quad (2)$$

where S_i is the luminescence signal at the wavelength λ_i , T_i is the transmission of the monochromator at the i th- λ value, and $\Delta(\lambda_i)$ is a constant Δ and wavelength interval at λ_i .

According to Beer's law for a single-ion-absorption, the absorbed power for the i th-channel is proportional to:

$$P_i = P_{0i} [1 - \exp(-\bar{\kappa}_i d)], \quad (3)$$

where $\bar{\kappa}_i$ is the average absorption coefficient ($\bar{\kappa}_i = \sigma_i N_i$, where σ_i is the absorption cross-section and N_i is the dopant concentration) and d is the crystal thickness.

The total absorbed power is given by:

$$P_t = \sum_i P_i. \quad (4)$$

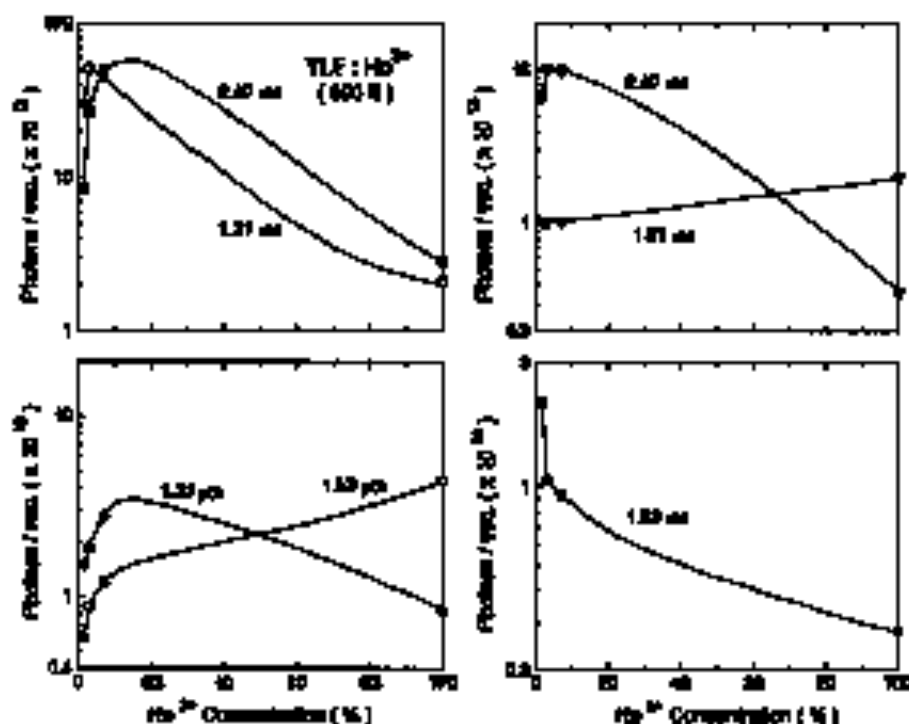


Fig. 2. Number of channels excited by the Ho^{3+} 5I₆ laser transition channels as a function of Ho concentration, for the Ho:YLF crystal under a Xe lamp spectrum at 300 K. The Ho^{3+} transitions corresponding to each curve are: 1.80 μm ($^5F_5 \rightarrow ^3F_4$), 1.21 μm ($^5F_5 \rightarrow ^3F_4$), 1.23 μm ($^5F_5 \rightarrow ^3F_4$), 1.51 μm ($^5F_5 \rightarrow ^3F_4$), 1.86 μm ($^5F_5 \rightarrow ^3F_4$), 2.03 μm ($^5F_5 \rightarrow ^3F_4$) and 0.40 μm ($^5F_5 \rightarrow ^3F_4$).

where Σ_{ν} is the summation over all the excited transitions for $\lambda \leq 1000$ nm.

3. Results

Using the Eq. (2) in Eq. (1) one obtains the equivalent power for each luminescent channel of Er^{3+} and Ho^{3+} ions. Dividing the power of one channel by its average photon energy, one gets the number of excited photons per second corresponding to that luminescent channel. The same procedure was adopted for all the luminescent channels studied in this work. Figs. 4 and 5 show the number of photons/s per luminescent channel, for several Er- and Ho-concentrations in YLF crystals. All the measurements were performed at room temperature since lasers working at low temperatures are more complicated to be operated, and as one always expects to see a laser which works really at room temperature.

4. Discussion and conclusions

4.1. Er^{3+} :YLF crystals

4.1.1. Luminescent transitions from the ${}^4S_{3/2}$ and ${}^4F_{9/2}$ laser levels

Fig. 4 shows that for low Er-concentration, i.e. from 1 to 2%, the Er^{3+} ion-level laser transitions most favored at room temperature are: 0.85, 1.11, 1.23, and 1.72 μm . For those transitions the number of photons/s as a function of the Er-concentration peaks at 1.2%, showing that the cross-relaxation processes are very efficient for concentrations above 1.7%, causing the decrease of the population from the ${}^4S_{3/2}$ and ${}^4F_{9/2}$ levels. When the ion transmittance increases from a very low value up to 2%, the excited power and the emission spectrum of the ${}^4S_{3/2}$ and ${}^4F_{9/2}$ levels increase. As a consequence, the number of photons emitted by those levels also increase. On the other hand, concentrations above 2% favor the cross-relaxation processes, which depopulate those levels, first producing the maximum luminescence peak for about 1.7% of Er in LYF crystals and a drastic decrease above this concentration.

Some authors [17–20] studied only the ${}^4S_{3/2}$ life

time as a function of the Er concentration for the $\text{LY}_{1-x}\text{Er}_x\text{F}_6$ (where $x = 0.01$ –1.00) crystals. Tlachuk et al. [17] indicated that an optimum Er concentration range for the laser transitions at 0.85 and 1.23 μm is 2 to 3% of $\text{Er}:\text{LYF}$ crystals, due to the ion-ion cross-relaxation processes which quench the ${}^4S_{3/2}$ luminescence. Barnes [18] pointed out that (6%)Er is the most appropriate concentration for a particular Q-switched Er:YLF pulsed laser at 1.73 μm . Pollock et al. [19] used a (3%)Er:YLF crystal to obtain laser action at 0.85, 1.23, and 1.73 μm by upconversion processes. Kirtz et al. [20] observed that the laser transition at 1.73 μm is not affected by a concentration of (2%)Er. On the other hand, concentrations \geq (4%)Er quench the ${}^4S_{3/2}$ luminescence and for a (16%)Er crystal, that laser level is completely quenched. The results presented by Kirtz et al. [20] are the closest to the present work (see Fig. 4) for the transitions from the ${}^4S_{3/2}$ laser level. We observed a similar behavior for the transition at 1.11 μm (${}^4F_{9/2} \rightarrow {}^4I_{13/2}$), peaking at (1.7%)Er, which was not studied before, at least in our knowledge.

4.1.2. Luminescent transitions from the ${}^4I_{11/2}$ and ${}^4I_{13/2}$ laser levels

Fig. 4 also shows that the emission at 1.62 μm is favored in the 25–35% Er-concentration range, and for the laser transition at 2.74 μm , an Er-doped YLF with 30–40% should be the most convenient candidate.

Studying the Er:YLF emission at 1.62 μm , we observed that the number of photons per second emitted by that channel increased more than for the (30.5%)Er:YLF system in comparison to the 1% Er-doped one, while the total excited power (for white light excitation) increased only by a factor of two. It starts to drop out because the Er concentration, the cross-relaxation transfers the population from the ${}^4S_{3/2}$ and ${}^4F_{9/2}$ levels to the ${}^4I_{11/2}$ and ${}^4I_{13/2}$ ones, reducing the number of photons emitted by the latter levels by a factor of ~ 4.5 .

It was also observed that for the ${}^4I_{13/2} \rightarrow {}^4I_{15/2}$ transition at 1.62 μm and, ${}^4I_{11/2} \rightarrow {}^4I_{13/2}$, at 2.74 μm , the curves corresponding to the number of photons (see Fig. 4) emitted per second as a function of the dopant-concentration show a pronounced initial increase, followed by a maximum for the concen-

tration range from 20 to 40%, and then slightly decreasing for higher Er concentrations.

According to Anzel et al. [21] the $^4I_{11/2}$ and $^4I_{13/2}$ laser level lifetimes are almost constant for concentrations up to (20%)Er, decreasing rapidly for concentrations higher than (25%)Er, because of the quenching processes to higher energy levels, coupling losses during the 3 μm laser action in Er:YLF. Sanderich et al. [22] studied the concentration of ions in the laser excitation at 3 μm for Er:YAG on the concentration range from 6.1 to 100%. Their conclusions are very similar to the ones from Anzel however, the authors mentioned the impurities quenching observed to occur irrespective with concentrations increase with the increase of Er concentration for $\geq 20\%$ (Er).

We observed a luminescence emission behavior for concentrations $\geq 10\%$ (Er), for the transitions at 3.74 μm and at 1.62 μm (see Fig. 4), which is captured if $\alpha_{sp}d \gg 1$ in Eq. (3), i.e., this condition is satisfied for this concentration level. The decrease in the number of photons/s for concentrations above 40% shows that there are some quenching processes occurring. In a previous publication [13,14] we attributed this quenching process to the energy transfer from the levels $^4I_{11/2}$ and $^4I_{13/2}$ of Er^{3+} ions and from the 3I_4 and 3I_2 of Ho^{3+} ions to the molecular impurities $\text{Mg}^{2+}(\text{OH}^-)$ and CHCO^- present in the crystal lattice.

Other effects such as self-quenching or upconversion, besides the energy transfer to sink impurities, must be considered in order to estimate the effective gain of the Er or Ho:YLF laser, medium to high concentrations. Particularly, taking into account all the considerations above, we can infer that for the Er laser excitation at 3.74 μm , the ideal concentration range is $10\% \leq x \leq 20\%$ (where x is the Er concentration).

4.2. Ho^{3+} :YLF crystals

From Fig. 3 one verifies that the most intense luminescence of Ho^{3+} ions are: 1.21 μm ($^2I_6 \rightarrow ^3I_4$), 2.06 μm ($^3I_2 \rightarrow ^3I_4$), 2.40 μm ($^3F_3 \rightarrow ^3I_3$). While the transitions at 1.00 and at 1.51 μm increase with the Ho concentration, the other luminescence decrease.

The 2.06 μm luminescence ($^3I_2 \rightarrow ^3I_4$) of the

Ho^{3+} :YLF crystal is maximized for concentrations in the range from 10 to 15%. Since this transition represents a three-level laser, such a high concentration would not help to improve the laser action because of the upconversion processes which adds a lot of population to the higher Ho levels, increasing the losses of the laser medium. To solve this problem a sensitizer is added to the host, generally Er or Tm ions, which efficiently transfer energy to the upper laser level 3I_2 .

For the transition $^3I_2 \rightarrow ^3I_4$, at 1.21 μm , the local concentration was in the range from 3 to 7%. The transition $^3S_2 \rightarrow ^3I_2$, at 1.35 μm , points out the range from 8 to 15%(Ho), decreasing for higher concentration. The transition $^3F_3 \rightarrow ^3I_3$, at 2.40 μm , is favored for Ho concentration between 7 and 10%. The other transitions coming from the 3F_3 laser level ($^3F_3 \rightarrow ^3I_2$ and $^3F_3 \rightarrow ^3I_4$) just increase with the concentration. The luminescence $^3I_2 \rightarrow ^3I_4$, at 1.66 μm , decreases all the way when the Ho concentration is increased. The transition at 2.5 μm , $^5I_4 \rightarrow ^3I_4$, was too weak to be observed in our experimental setup.

According to Thakurik et al. [23] under a weak lamp pumping for a Ho:YLF crystal, the laser level 3S_2 , 3I_2 , and 3I_3 are self-quenched with the increase of the Ho concentration. For a Ho:LF crystal, under a strong lamp pumping, there is an energy migration to the long-lived levels 3I_4 and 3I_2 , and the interaction processes between excited ions as well as the non-linear processes due to the pumping intensity have to be taken into account. If one compares the Ho:LF crystal with the activated one Ho^{3+} :YLF, that condition improves the stimulated emission generation on the $^3F_3 \rightarrow ^3I_j$ ($j = 2, 6, 7$) whereas the (3S_2 , 3F_3) laser becomes non-stimulated and no lasing is observed. Particularly, the presence of cross-relaxation interaction is related to the absence of lasing for the transition $^3I_6 \rightarrow ^3I_2$, at 3.00 μm , for the Ho:LF crystal and to the possibility of obtaining laser from the short-lived multiplet 3F_3 for the transitions $^3F_3 \rightarrow ^3I_j$ ($j = 2, 6, 7$).

We observe that the behavior of fluorescence intensities from the level 3F_3 at 1.00 and 1.51 μm (see Fig. 5) with the increase of the Ho concentration are in agreement with Thakurik's data, but the maximum at 2.40 μm from the same laser level showed a different behavior, exhibiting a short range of maximization. Also in agreement with that paper are the

transitions coming from the levels 3I_0 and 3I_1 to the ground-state 3I_0 and the one from 3I_2 to 3I_1 . These transitions suffer a very strong quenching in its luminescence, and since the first two are transitions to the ground state, they should not be efficient unless the Ho ions are sensitized by donors.

In conclusion, although this method is a good approach to determine the local RE^{3+} -concentration for a four-level laser transition system, it is not very convenient for a three-level laser such as the case at 1.62 μm (Er:YLF) and at 2.06 μm (Er:YLF). For the latter case, the method is useful to study the ion luminescence behavior. Concerning the laser action of a three-level system, one needs to consider the laser catheter gain and the losses due to the non-laser processes, which have a strong dependence on the activator concentration. Indeed, the laser gain of a three-level laser is very low for a high dopant concentration ($> 2 \times 10^{20}$) since a significative fraction of activator population remains in the lowest Stark level from the ground-state at room temperature, precluding the population inversion and creating problems to achieve the threshold.

Acknowledgements

The authors would like to thank FINEP, CNPq/UEAE and FAPESP, from Brazil, for their financial support.

References

- [1] C.E. Desl. Conference on Lasers and Electro-Optics, 1983 Technical Digest, Vol. 15 OPA, Baltimore, MD paper CTu2, p. 51.
- [2] L. Dori and T. Javoz, Opt. Lett. 10 (1985) 134.
- [3] D.R. Jacobs, IEEE J. Quantum Electron. 20 (1984) 2617.
- [4] J.L. Dutton, Opt. Opt. 33 (1990) 6373.
- [5] J.P. Fies, L. Escamez and G. Henseler, Conf. on Lasers and Electro-Optics, 1989 Technical Digest, Vol. 13 OPA, Baltimore, MD paper CTu2, p. 130.
- [6] R. Reed, IEEE Circ. Dev., May (1971).
- [7] B.N. Anagnost, B.S. Drazdov, A.V. Lohm, V.V. Lyubchikov, A.V. Zhukovskiy and V.I. Tarasov, Sov. J. Opt. Technol. 66 (1989) 418.
- [8] J.P. Conroy and J.T. Walsh, Jr., Opt. Phys. Lett. 63 (1987) 1983.
- [9] D.E. Johnson, G. Crivello and M.E. Fehn, Laser Eng. Med. 12 (1992) 393.
- [10] M.E. Chavira, B.D. Stone and M. Stutzman, Opt. Lett. 20 (1992) 336.
- [11] M.E. Chavira, B.D. Stone and M. Stutzman, Appl. Phys. Lett. 65 (1992) 2948.
- [12] M.E. Chavira, L. Gomez and J.P. Morton, Opt. Mater. 4 (1993) 327.
- [13] L.J. Chiriac, L. Gomez and J.P. Morton, Phys. Rev. B 51 (1995) 2064.
- [14] M.E. Chavira, Manus. Electronics and Systems Center, USC Technology, Berkeley, CA.
- [15] A. D'Alia de Fiumicino, Ph.D. Thesis, USC, Los Angeles, CA, 1993.
- [16] A.M. Tsvetkov, M.V. Pavlov, M.L. Krut'kov and G. Krut'kova, Sov. Phys. Tech. Phys. 35 (1990) 337.
- [17] H. Shimizu, Laser Raman Technology and Applications, SPIE, Vol. 258 (1980).
- [18] S.A. McPhail, G.R. Cheng and M. Stutzman, Appl. Phys. Lett. 34 (1990) 669.
- [19] G. Hensler, L. Escamez and M. Stutzman, Topical Meeting on Opt. Vol. Lasers, Oct. 26-30, 1987, Techn. Dig., 215, paper WED-1.
- [20] S. Hase, G. Matsuoka, B.H. Stein and P. Ancl. J. Lasers 69 (1991) 7.
- [21] R. Gumprecht, V. Lapan, A. Lapan, V.I. Shchegol, Y.M. Shchegol and M.L. Stutzman, Opt. Commun. 61 (1992) 139.
- [22] A.K. Tsvetkov, M. Krut'kova and M.V. Pavlov, Opt. Spectrosc. (USSR) 26 (1985) 623.